

# Conductivity imaging with a single measurement of boundary and interior data

Adrian Nachman<sup>†</sup> , Alexandru Tamasan<sup>‡</sup> , and Alexandre Timonov<sup>§</sup>

<sup>†</sup> Department of Mathematics and the Edward S. Rogers Sr. Department of Electrical and Computer Engineering, University of Toronto, Toronto, Ontario, Canada

E-mail: [nachman@math.toronto.edu](mailto:nachman@math.toronto.edu)

<sup>‡</sup> Department of Mathematics, University of Central Florida, Orlando, FL, USA

E-mail: [tamasan@math.ucf.edu](mailto:tamasan@math.ucf.edu)

<sup>§</sup> Division of Mathematics and Computer Science, University of South Carolina Upstate, Spartanburg, SC, USA

E-mail: [atimonov@uscupstate.edu](mailto:atimonov@uscupstate.edu)

**Abstract.** We consider the problem of imaging the conductivity from knowledge of one current and corresponding voltage on a part of the boundary of an inhomogeneous isotropic object and of the magnitude  $|J(x)|$  of the current density inside. The internal data is obtained from Magnetic Resonance measurements. The problem is reduced to a boundary value problem with partial data for the equation  $\nabla \cdot |J(x)| |\nabla u|^{-1} \nabla u = 0$ . We show that equipotential surfaces are minimal surfaces in the conformal metric  $|J|^{2/(n-1)} I$ . In two dimensions, we solve the Cauchy problem with partial data and show that the conductivity is uniquely determined in the region spanned by the characteristics originating from the part of the boundary where measurements are available. We formulate sufficient conditions on the Dirichlet data to guarantee the unique recovery of the conductivity throughout the domain. The proof of uniqueness is constructive and yields an efficient algorithm for conductivity imaging. The computational feasibility of this algorithm is demonstrated in numerical experiments.

## 1. Introduction

Traditionally, in Electrical Impedance Tomography (EIT) one seeks to determine the conductivity inside an object from boundary measurements of multiple currents and corresponding voltages. The sensitivity of the boundary data to variations of the conductivity inside the object has been shown to be very low [5], [9], resulting in images with resolution which deteriorates away from the boundary.

In this paper we consider a different kind of inverse problem, where in addition to boundary data one has knowledge of the magnitude of one current density field inside. Such information can be obtained from magnetic resonance measurements, as first shown in [16]. When two current density fields are known, an isotropic conductivity can be recovered in regions where the fields are transversal via an explicit local formula [10], [13]. When the magnitudes of two currents are given, one can uniquely determine the singular support of the conductivity distribution as shown in [11]. Moreover, a numerical reconstruction can be obtained via the so called  $J$ -substitution algorithm [12], which uses two injected currents. The latter works combined Ohm's law  $J = -\sigma \nabla u$  with the charge conservation law  $\nabla \cdot J = 0$  to obtain the quasi-linear differential equation

$$\nabla \cdot \left( \frac{|J|}{|\nabla u|} \nabla u \right) = 0. \quad (1.1)$$

Some examples of non-uniqueness and non-existence of the solution to the Neumann problem for this equation were given in [11]. This showed that Neumann boundary data and the magnitude of one current density are insufficient to determine the conductivity.

The problem that we study in this paper is whether knowledge of the magnitude  $|J|$  of one current density inside the domain together with the corresponding Cauchy data on a part of the boundary is sufficient to determine the conductivity. For planar domains we show that, in general, such data can determine the conductivity in a specific subregion of the domain and cannot determine the conductivity elsewhere. We also identify sufficient conditions which ensure that the conductivity is recovered in the whole domain.

We begin this paper with a geometric result (Theorem 2.1) valid in all dimensions  $n \geq 2$ : The equipotential surfaces have zero mean curvature in the conformal metric  $|J|^{2/(n-1)} I$  given by the magnitude of the current density. In two dimensions, the equipotential lines are geodesics in this metric. Moreover, they can also be viewed as characteristics of the equation (1.1), which is parabolic according to the classical classification. One can find the geodesics originating on the part of the boundary where measurements are available by solving an initial value problem for a family of nonlinear ordinary differential equations. The voltage potential  $u$  is determined in the region spanned by these characteristics and the conductivity can then be calculated as  $\sigma = |J|/|\nabla u|$ .

We are able to prove global uniqueness (Theorem 3.1) and conditional stability (Theorem 3.2) results for a specific class of voltage distributions on the boundary. The proof is constructive. It is used when developing the reconstruction algorithm. The last section demonstrates the computational feasibility of this algorithm on synthetic data.

## 2. Equipotential surfaces as minimal surfaces in a conformal metric

Let  $\Omega \subset R^n$  be an open set endowed with the conformal metric  $g = aI$  for some conformal factor  $a \in C^1(\Omega)$ ,  $a > 0$ . The length of a vector  $v$  in the  $g$ -metric is denoted by  $|v|_g$ , whereas for the Euclidean length we use  $|v|$ .

**Lemma 2.1.** *Let  $u \in C^1(\Omega)$  be such that  $|\nabla u| > 0$ . Then the level sets of  $u$  are  $C^1$ -surfaces of mean curvature*

$$H = \pm \frac{1}{a^{n/2}} \nabla \cdot \left( a^{\frac{n-1}{2}} \frac{\nabla u}{|\nabla u|} \right). \quad (2.1)$$

**Proof.** From the implicit function theorem we know that the level sets are  $C^1$ -smooth surfaces. The mean curvature of a surface with the unit normal  $\nu_g$  is given by  $H = \operatorname{div}_g(\nu_g)$ , where

$$\operatorname{div}_g(\cdot) = \frac{1}{\sqrt{\det g}} \sum_i \partial_i (\sqrt{\det g}(\cdot)_i), \quad \nu_g = \frac{g^{-1}\nu}{|g^{-1}\nu|_g} \quad (2.2)$$

and  $\nu$  is the Euclidean unit normal (see, e.g., [7]). In the conformal case, we have  $\det g = a^n$ ,  $g^{-1}\nu = a^{-1}\nu$  and  $|v|_g = \sqrt{a}|v|$  for any vector  $v$ . Therefore  $|g^{-1}\nu|_g = \sqrt{a}/a|\nu| = 1/\sqrt{a}$ . If the surface is a level set of  $u$  then  $\nu = \pm \nabla u / |\nabla u|$  and  $\nu_g = \pm \frac{1}{\sqrt{a}} \frac{\nabla u}{|\nabla u|}$ . Substituting this formula into the equation (2.2) we obtain (2.1).  $\square$

**Theorem 2.1.** *Let  $u \in C^1(\Omega)$  be an electric potential with current density  $J$ . If  $J \neq 0$  in  $\Omega$ , then the level sets  $u = c$  are surfaces of zero mean curvature in the conformal metric  $g = |J|^{2/(n-1)}I$ . Moreover, they are critical surfaces for the functional*

$$E(\Sigma) = \int_{\Sigma} |J| dS, \quad (2.3)$$

where  $dS$  is the Euclidean surface measure.

**Proof.** Take  $a = |J|^{2/(n-1)}$  in (2.1). The nonlinear equation (1.1) satisfied by  $u$  is equivalent to  $H = 0$ .

Consider now a local parametrization of  $\Sigma_c = \{x \in \Omega : u = c\}$  given by  $\{(x', \psi(x', c)) : x' \in U\}$  for some open  $U \subset R^{n-1}$ . The formula for the functional (2.3) becomes

$$E(\psi(\cdot, c)) = \int_U |J|(x', \psi(x', c)) \sqrt{1 + |\nabla' \psi(x', c)|^2} dx', \quad (2.4)$$

where  $\nabla'$  denotes the gradient in the first  $n-1$  variables. The Euler-Lagrange equation for the functional above is

$$\nabla' \cdot \left( \frac{|J|(x', \psi(x', c)) \nabla' \psi(x', c)}{\sqrt{1 + |\nabla' \psi(x', c)|^2}} \right) = \frac{\partial |J|}{\partial x_n}(x', \psi(x', c)) \sqrt{1 + |\nabla' \psi(x', c)|^2}. \quad (2.5)$$

Along the surface  $\Sigma_c$ , the partial derivatives of  $u$  are calculated from the derivatives of  $\psi$  by implicit differentiation in  $u(x', \psi(x', c)) = c$ :

$$\begin{aligned} u_{x_i} &= -\psi_{x_i}/\psi_c, \quad u_{x_n} = 1/\psi_c, \\ u_{x_i x_j} &= (\psi_{x_j c} \psi_{x_i} \psi_c + \psi_{x_i c} \psi_{x_j} \psi_c - \psi_{cc} \psi_{x_i} \psi_{x_j} - \psi_{x_i x_j} \psi_c^2) / \psi_c^3, \\ u_{x_i x_n} &= (\psi_{cc} \psi_{x_i} - \psi_{x_i c} \psi_c) / \psi_c^3, \\ u_{x_n x_n} &= -\psi_{cc} / \psi_c^3, \end{aligned} \quad (2.6)$$

for  $i, j = 1, \dots, n-1$ .

In the equation (1.1) at each point  $(x', \psi(x', c))$  on the surface  $\Sigma_c$  we replace the derivatives of  $u$  in terms of the derivatives of  $\psi$  from the formula (2.6). We obtain the family (indexed by  $c$ ) of the quasi-linear elliptic equations in  $x' = (x_1, \dots, x_{n-1})$

$$\begin{aligned} & (1 + |\nabla' \psi|^2)^{-1} \left( \sum_{i=1}^{n-1} (1 + |\nabla' \psi|^2 - \psi_{x_i}^2) \psi_{x_i x_i} - 2 \sum_{1 \leq i < j \leq n-1} \psi_{x_i} \psi_{x_j} \psi_{x_i x_j} \right) \\ & = \nabla \ln |J| \cdot (\nabla' \psi, 1). \end{aligned} \quad (2.7)$$

This is an equivalent form of (2.5).  $\square$

In the equation (2.7), the function  $\psi$  appears nonlinearly in  $\nabla \ln |J|(x', \psi(x', c))$ , but  $c$  appears as a parameter only. In two dimensional domains, the equation (2.7) is simplified as follows. On the set  $D_1 = \{(x, y) \in \Omega : u_y(x, y) \neq 0\}$ , an equipotential curve is a graph of the function  $\psi(x, c)$  that solves

$$\psi_{xx}(x, c) = \left( \psi_x^2(x, c) + 1 \right) \left[ -\frac{|J|_x}{|J|}(x, \psi(x, c)) \psi_x(x, c) + \frac{|J|_y}{|J|}(x, \psi(x, c)) \right]. \quad (2.8)$$

On the set  $D_2 = \{(x, y) \in \Omega : u_x(x, y) \neq 0\}$ , an equipotential curve is a graph of the function  $\phi(c, y)$  that solves

$$\phi_{yy}(s, y) = \left( \phi_y^2(s, y) + 1 \right) \left[ -\frac{|J|_y}{|J|}(\phi(s, y), y) \phi_y(s, y) + \frac{|J|_x}{|J|}(\phi(s, y), y) \right]. \quad (2.9)$$

### 3. Uniqueness and conditional stability

Throughout this section  $\Omega$  is assumed to be a simply connected planar domain with  $C^1$ -smooth boundary and  $\sigma \in L^\infty(\Omega)$  is a positive function. Further regularity on  $\sigma$  will be specified in the theorems. A  $\sigma$ -harmonic function is any solution  $u \in H^1(\Omega)$  of the conductivity equation

$$\nabla \cdot \sigma \nabla u = 0. \quad (3.1)$$

Consider the following coefficient identification problem: *Given the Cauchy data  $(u|_\Gamma, \partial_\nu u|_\Gamma)$  on an arc  $\Gamma$  of the boundary and the magnitude of the current density  $|J| = |\sigma \nabla u|$  in  $\Omega$ , find the conductivity  $\sigma$  in  $\Omega$ .*

We formulate sufficient conditions on the boundary data for the unique solvability of this problem. In some practical situations, such conditions can be satisfied.

**Definition 3.1.** A function  $f$  continuous on a simple closed contour will be called *almost two-to-one* if it is a two-to-one map, except possibly at its maximum and minimum.

There are exactly two maximal arcs on each of which the function  $f$  is strictly monotonic. The lemma below describes the geometry of the level sets of  $\sigma$ -harmonic maps  $u$  with almost two-to-one traces on the boundary. It is a consequence of Alessandrini's result on the index of critical points [1].

**Lemma 3.1.** *Let  $\Omega$  be a simply connected planar domain,  $\sigma \in C^\mu(\Omega)$ ,  $0 < \mu < 1$  and  $u$  be  $\sigma$ -harmonic in  $\Omega$  with  $u|_{\partial\Omega}$  almost two-to-one. Then  $|\nabla u| > 0$  in  $\bar{\Omega}$ , and each level set of  $u$  is a  $C^1$ -smooth curve inside  $\Omega$  with the two endpoints on the boundary.*

**Proof.** In two dimensions, the critical points of  $\sigma$ -harmonic functions are isolated. This is a consequence of the fact that  $(\partial_x + i\partial_y)u$  is pseudo-analytic. The regularity of  $\sigma$  implies that  $u \in C^1(\overline{\Omega})$  ( see, e.g., [17]). Alessandrini's result (Theorem 1.1, [1]) and our choice of boundary data imply that all possible critical points in  $\Omega$  have zero index, so that there are no critical points inside. The maximum principle implies that no critical points lie on the boundary either. It follows from the implicit function theorem that each level set is a one dimensional manifold with boundary. Loops cannot occur. Otherwise, by the maximum principle,  $u$  is constant in the region inside. Also, the level set cannot have an arc ending inside since such an endpoint would be a critical point. Each level set is thus one connected arc with endpoints on the boundary. Since each level set is compact in  $\overline{\Omega}$ , one can find a finite covering by closed balls, in each of which the set has finite length.  $\square$

**Theorem 3.1 [Unique determination].** *Let  $\Omega$  be a simply connected, bounded domain in the plane with piecewise  $C^1$ -smooth boundary. Let  $f \in C^2(\partial\Omega)$  be an almost two-to-one function and let  $\Gamma$  denote one of the maximal arcs on which  $f$  is strictly monotonic. Given  $g \in C^1(\Gamma)$  and  $|J| \in C^1(\overline{\Omega}) \cap C^2(\Omega)$ , there exists a unique pair  $(\sigma, u) \in C^2(\Omega) \times C^2(\Omega)$ , such that  $u$  is  $\sigma$ -harmonic and*

$$\begin{aligned}\sigma|\nabla u| &= |J|, \\ u|_{\Gamma} &= f|_{\Gamma}, \\ \partial_\nu u|_{\Gamma} &= g.\end{aligned}$$

**Proof.** For  $\sigma \in C^2(\Omega)$  we show that all equipotential curves can be traced inside  $\Omega$  starting from points on  $\Gamma$ . By choosing a curvilinear coordinate system with  $y$  along  $\Gamma$  and  $\partial_x$  transversal, without loss of generality, we consider  $\Gamma$  to be the straight segment  $\{0\} \times [0, 1]$ . From the lemma 3.1 we have that  $|\nabla u| > 0$  in  $\overline{\Omega}$  and the level curves can be locally described by the graphs of functions in  $x$  or of functions in  $y$ . For each  $t \in (f(0), f(1))$  the Cauchy data  $u(0, y) = f(y)$  and  $u_x(0, y) = g(y)$  determine the initial data for  $\psi(\cdot, t)$  via

$$\begin{aligned}\psi(0, t) &= f^{-1}(t), \\ \psi_x(0, t) &= -\frac{g}{f'} \circ f^{-1}(t).\end{aligned}\tag{3.2}$$

Since  $u_y(0, y) = f'(y) > 0$ , we have that  $u_y > 0$  in an open neighborhood of  $\Gamma$ . Since  $|J| \in C^1(\overline{\Omega}) \cap C^2(\Omega)$ , the right-hand side of equation (2.8) is Lipschitz in  $\psi$ . From classical results on the existence and uniqueness theory for initial value problems for differential equations (see, e.g., [6], [8]), the equation (2.8) subject to the initial conditions (3.2) has a unique solution in a maximal interval  $[0, h_+(t))$ . Moreover, for each  $x \in [0, h_+(t))$ ,  $\psi(x, \cdot) \in C^1(f(0), f(1))$ . As  $x \rightarrow h_+(t)$ , we have that either  $(x, \psi(x, t))$  reaches the boundary  $\partial\Omega$  or, at least on a sequence  $x_n \rightarrow h_+$ ,  $\psi_x(x_n, t)$  blows up. If the solution reached the boundary  $\partial\Omega$ , we are done. Otherwise,  $\lim_{n \rightarrow \infty} \psi_x(x_n, t) = \infty$ , and from (2.6) we have  $u_y(h_+, \psi(h_+, t)) = 0$ . Since  $\nabla u$  never vanishes, then  $u_x(h_+, \psi(h_+, t)) \neq 0$  and the equipotential line is the graph of a function

in  $y$ . This function can be found by solving the initial value problem for (2.9) subject to the initial conditions

$$\begin{aligned}\phi(t, 0) &= h_+, \\ \phi_y(t, y) &= 0.\end{aligned}\tag{3.3}$$

As before, we can trace the equipotential line until we either reach the boundary or we reach a point where  $u_x$  vanishes. In the latter situation, we switch back to solving another initial value problem for  $\psi(x, t)$  in (2.8), which starts at the current position with zero initial velocity. The graph parametrization implies that we traced the equipotential line with super-unitary speed. Since the total length is finite, this process ends after finitely many steps.

The choice of  $\Gamma$  and the maximum principle ensure that any interior point lies on an equipotential line reaching the boundary on  $\Gamma$ . Therefore any interior point lies on one equipotential line reaching the boundary on  $\Gamma$  and thus  $u$  is uniquely determined at all points in  $\Omega$ . Moreover, since  $\psi$  or  $\phi$  are  $C^1$  in both variables where defined, we get  $u \in C^1(\Omega)$ . The conductivity is found by the formula

$$\sigma = \frac{|J|}{|\nabla u|}.\tag{3.4}$$

□

The result given below shows that, in general, outside the region spanned by the characteristics originating on  $\Gamma$  we have non-uniqueness. For each  $0 < h \leq 1$  and  $0 < c \leq 1$  we introduce the domains

$$\Omega_{h,c} = \left\{ (x, y) : x \in (0, h), 0 < y < \frac{c}{x+1} \right\}.$$

**Proposition 3.1.** [Non-uniqueness] *There exist  $h > 0$  and a domain  $\Omega \supset \Omega_{h,1/2}$ , such that the equation (1.1) with  $|J|(x, y) = \sqrt{(x+1)^2 + y^2}$  has at least two different solutions in  $\Omega$ , both satisfying the Cauchy conditions  $u(0, y) = u_x(0, y) = y$  for  $0 \leq y \leq 1/2$ . These solutions represent voltages for two different conductivities while generating internal current density fields of the same magnitude.*

**Proof.** We first notice that  $\tilde{u}(x, y) = (x+1)y$  is a solution of (1.1) in  $\Omega_{1,1}$  that satisfies the boundary conditions on  $\{0\} \times [0, 1/2]$ . Next, we construct a different solution in a sub-domain of  $\Omega_{1,1}$ . To simplify notations, let

$$\begin{aligned}\mathcal{L}[\psi](x, c) &= \psi_{xx}(x, c) - \left( \psi_x^2(x, c) + 1 \right) \left[ -\frac{|J|_x}{|J|}(x, \psi(x, c))\psi_x(x, c) \right. \\ &\quad \left. + \frac{|J|_y}{|J|}(x, \psi(x, c)) \right],\end{aligned}$$

(see the equation (2.8)).

For  $c, h \in (0, 1)$  consider the family of boundary value problems

$$\mathcal{L}[\psi](x, c) = 0, \psi(0, c) = c, \psi(h, c) = \frac{1}{h+1} \left( c + h \max \left\{ 0, c - \frac{1}{2} \right\}^3 \right).$$

From the theory of ordinary differential equations (see, e.g., [8]), there exists a sufficiently small  $h > 0$ , such that for each  $c \in [0, 1]$  the corresponding problem has

a unique solution in  $x \in [0, h]$ . Moreover, since the boundary data is  $C^2$ -smooth in the parameter  $c$  and the equation is independent of  $c$ , we have that  $\psi \in C^2((0, h) \times (0, 1))$ . Let  $\tilde{\psi}(x, c) = c/(x+1)$ . For  $c \in [0, 1/2]$ , one can check that  $\psi(x, c) = \tilde{\psi}(x, c)$ . Since  $\psi_c(x, 1/2) \geq 1/(h+1) > 0$  for every  $x \in [0, h]$  due to the uniform continuity in  $c$  of  $\psi_c$ , we have that  $\psi_c(x, c) \geq 1/2(h+1) > 0$  when  $c \leq \epsilon + 1/2$  for some  $\epsilon > 0$ . Note that  $\psi(h, c) > \tilde{\psi}(h, c)$  for  $1/2 < c < 1/2 + \epsilon$ . Since the boundary value problem for  $\mathcal{L}[\psi] = 0$  has a unique solution on  $[0, h]$  for any  $0 < h_1 < h$ , it follows that  $\psi(x, c) > \tilde{\psi}(x, c)$  for all  $x$ ,  $0 < x < h$ , and

$$\psi_x(0, c) > \tilde{\psi}_x(0, c). \quad (3.5)$$

On the domain  $\Omega = \{(x, \psi(x, c)) : x \in (0, h), c < 1/2 + \epsilon\}$  we define

$$u(x, y) = \psi(x, \cdot)^{-1}(y). \quad (3.6)$$

The domain  $\Omega$  contains  $\Omega_{h, 1/2}$  and the restriction of  $u$  to  $\Omega_{h, 1/2}$  is equal to  $\tilde{u} = (x+1)y$ . Following its definition in (3.6) and using the implicit differentiation as in (2.6), we calculate

$$\frac{|\nabla u|^3}{|J|} \nabla \cdot \left( \frac{|J|}{|\nabla u|} \nabla u \right) (x, \psi(x, c)) = \frac{1}{\psi_c^3(x, c)} \mathcal{L}[\psi](x, c) = 0.$$

Therefore, the function  $u$  defined in (3.6) solves the equation (1.1) in  $\Omega$  and satisfies the boundary conditions  $u(0, y) = u_x(0, y) = y$  for  $y \in [0, 1/2]$ . Comparing the level sets  $y = \psi(x, c)$  and  $y = \tilde{\psi}(x, c)$  of  $u$  and  $\tilde{u}$ , respectively, we see that  $u(x, y) < \tilde{u}(x, y)$  for  $(x, y) \in \Omega$ ,  $y > 1/2(h+1)$ .

We now show that for a sufficiently small  $\tilde{\epsilon} > 0$ ,  $|\nabla u(0, y)| \neq |\nabla \tilde{u}(0, y)|$ ,  $y \in (1/2, 1/2 + \epsilon)$ . Assume the opposite, i.e.,  $|\nabla u(0, y)| = |\nabla \tilde{u}(0, y)|$ . Then since  $u_y(0, y) = \tilde{u}_y(0, y) = 1$  for  $y \in (0, 1/2 + \epsilon)$ , we have  $u_x(0, y) = \pm \tilde{u}_x(0, y)$ . Also,  $\tilde{u}_x(0, y) = y \geq 1/2$ , so that by virtue of the continuous dependence of solutions to the equation (2.8) on the data, we obtain  $u_x(0, h) > 0$ ,  $h \in (1/2, 1/2 + \tilde{\epsilon})$  for a sufficiently small  $\tilde{\epsilon}$ . Therefore, we would have  $u_x(0, y) = \tilde{u}_x(0, y)$ ,  $y \in (1/2, 1/2 + \tilde{\epsilon})$  and  $\psi(0, c) = \tilde{\psi}(0, c)$  and  $\psi_x(0, c) = \tilde{\psi}_x(0, c)$ , contradicting (3.5). We then conclude that since  $u$  and  $\tilde{u}$  share the same  $|J|$ , they correspond to conductivities  $\sigma = |J|/|\nabla u|$  and  $\tilde{\sigma} = |J|/|\nabla \tilde{u}|$ , which differ in a neighborhood of the segment  $\{0\} \times (1/2, 1/2 + \tilde{\epsilon})$ .  $\square$

Based on the classical results of continuous dependence on the data of solutions of ordinary differential equations, we now show that the reconstruction is conditionally stable. Let  $u, \tilde{u}$  be two admissible  $\sigma$ -harmonic, respectively  $\tilde{\sigma}$ -harmonic maps and let

$$u|_{\Gamma} = f, \tilde{u}|_{\Gamma} = \tilde{f}, |J| = \sigma |\nabla u| \partial_{\nu} u|_{\Gamma} = g, \partial_{\nu} \tilde{u}|_{\Gamma} = \tilde{g}, |\tilde{J}| = \tilde{\sigma} |\nabla \tilde{u}|.$$

Let

$$M = \max\{\|\nabla \ln |J|\|_{C^1(\bar{\Omega})}, \|\nabla \ln |\tilde{J}|\|_{C^1(\bar{\Omega})}\}. \quad (3.7)$$

Denote  $\|\cdot\|_{\infty}$  the sup-norm in  $\bar{\Omega}$ , and  $\|u\|_{C^1(\bar{\Omega})} = \|u\|_{\infty} + \|\nabla u\|_{\infty}$ .

**Theorem 3.2 [Conditional Stability].** *Let  $\Omega$  be a simply connected domain with smooth boundary and  $f, \tilde{f} \in C^2(\partial\Omega)$  be almost two-to-one maps which have a common maximal arc  $\Gamma$ . Assume that*

$$\inf_{\Gamma} f' \geq \epsilon, \inf_{\Gamma} \tilde{f}' \geq \epsilon$$

and

$$\max\left\{\left\|\frac{g}{f'} - \frac{\tilde{g}}{\tilde{f}'}\right\|_{C^1(\Gamma)}, \|f^{-1} - \tilde{f}^{-1}\|_{C^1(\Gamma)}, \|\nabla(\ln|J| - \ln|\tilde{J}|)\|_{C^1(\bar{\Omega})}\right\} \leq \eta$$

for some  $\eta > 0$ . Then

$$\|\sigma - \tilde{\sigma}\|_{\infty} \leq \Phi(\eta),$$

where  $\Phi : [0, \infty) \rightarrow [0, \infty)$  is a map depending on  $\epsilon, M$  and  $\|\tilde{\sigma}\|_{\infty}$ ,  $\|\tilde{g}/\tilde{f}'\|_{\infty}$ ,  $\|\tilde{f}^{-1}\|_{\infty}$  with  $\lim_{\eta \rightarrow 0} \Phi(\eta) = 0$ .

**Proof.** It suffices to perform all the estimates locally around each point  $Q_0 = (x_0, y_0) \in \Omega$ . To fix ideas, let us assume that  $u_x(x_0, y_0) \neq 0$ . Thus, the equipotential curve of  $u$  passing through  $Q_0$  is locally the graph of a function of  $x \rightarrow \psi(x, t)$ , and from (2.6) we have for some  $\delta > 0$  that

$$0 < \delta \leq |\nabla\psi| \leq \delta^{-1} < \infty$$

near  $Q_0$ . Due to the continuous dependence of solutions of the initial value problems on the data (see, e.g., [6], [8]), we also have

$$0 < \delta \leq |\nabla\tilde{\psi}| \leq \delta^{-1} < \infty$$

in a (possibly smaller) neighborhood of  $Q_0$ . The equipotential curve of  $\tilde{u}$  passing through  $Q_0$  is thus also the local graph of a function of  $x$ , i.e.  $Q_0 = (x_0, \psi(x_0, t_0)) = (x_0, \tilde{\psi}(x_0, \tilde{t}_0))$ , for some  $t_0, \tilde{t}_0 \in (f(0), f(1))$ , the corresponding potentials  $u$  and  $\tilde{u}$  at  $Q_0$ .

Since  $\|\psi_t\| \leq 1/\delta$  and  $|\nabla u| = \sqrt{\frac{\psi_x^2 + 1}{\psi_t^2}} \geq \frac{1}{|\psi_t|}$ , we have the estimate

$$\begin{aligned} |\sigma(x_0, y_0) - \tilde{\sigma}(x_0, y_0)| &= \left| \frac{|J|}{|\nabla u|} - \frac{|\tilde{J}|}{|\nabla \tilde{u}|} \right| (x_0, y_0) \\ &\leq \frac{1}{\delta} \left( \|J - \tilde{J}\|_{\infty} + \|\tilde{\sigma}\|_{\infty} \|\nabla u - \nabla \tilde{u}\|_{\infty} \right). \end{aligned}$$

The last term in this formula can be estimated by using the implicit differentiation formulae (2.6) as follows.

$$|\nabla u - \nabla \tilde{u}| \leq \sqrt{\left(\frac{\psi_x}{\psi_t} - \frac{\tilde{\psi}_x}{\tilde{\psi}_t}\right)^2 + \left(\frac{1}{\psi_t} - \frac{1}{\tilde{\psi}_t}\right)^2} \leq \frac{1}{\delta^2} \sqrt{\delta^2 + 1} \|\nabla\psi - \nabla\tilde{\psi}\|_{\infty}.$$

Classical results (see, e.g., [6, 8]) imply that  $\|\nabla\psi - \nabla\tilde{\psi}\|_{\infty}$  is of order  $O(\eta)$ . The result follows.  $\square$

Note that since  $\Phi$  depends on  $\|\tilde{\sigma}\|_{\infty}$ , this proof shows only conditional stability.

#### 4. Numerical experiments

To demonstrate the computational feasibility of the reconstruction algorithm, some numerical experiments were conducted. The computations were performed on a laptop PC with Pentium IV, 2.8 GHz CPU, 1 Gb of RAM, running under Windows XP. In programming, the Interactive Data Language †(IDL 6.2) was used. The time of

† Software product of Research Systems, Inc.



computations varied from a few minutes to an hour depending on both the grids and accuracy desired.

Two experiments are conducted. In the first experiment, the voltage is almost two-to-one on the boundary, whereas in the second one it is not.

#### 4.1. Simulation of the data

Let  $\Omega = (0, 1) \times (0, 1)$  be the unit square. The model conductivity is given by

$$\sigma(x, y) = 1 + \sigma_0(x, y),$$

where  $\sigma_0$  is a function with support in  $\Omega$  modelled by the CT-image of a human body. The density distribution in the original CT-image was rescaled to simulate the conductivity distribution in  $\Omega$  with values varying from 1 to 1.8 S/m. The simulated conductivity distribution in a human body is shown in Figure 1.

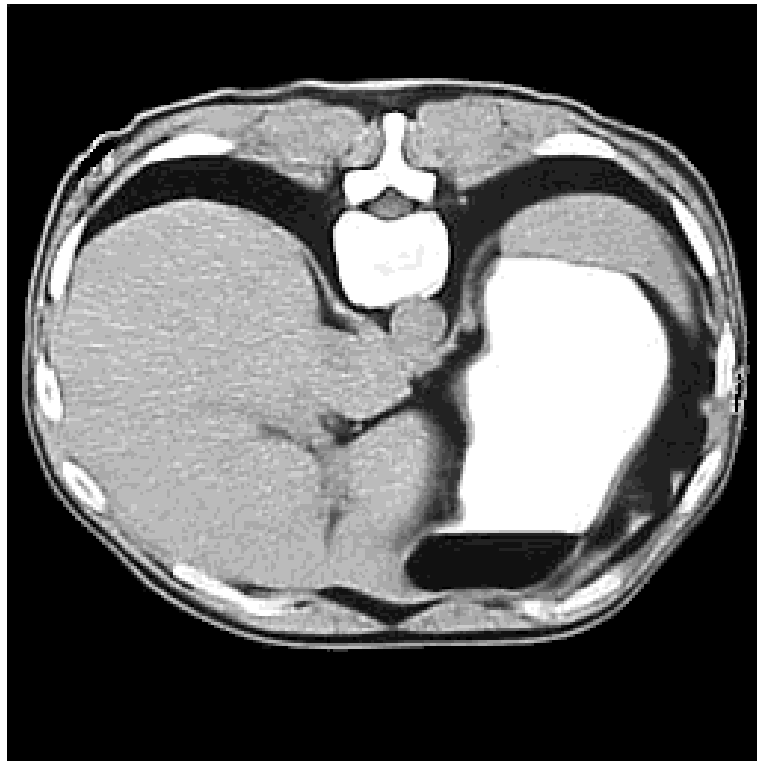


**Figure 1.** The original conductivity distribution.

In the first experiment, the data are generated from the numerical solution of the Dirichlet problem for the conductivity equation (3.1) in  $\Omega$  subject to the boundary conditions:  $u_1 = y$  on the vertical sides,  $u_1 = 1$  on the top side and  $u_1 = 0$  on the bottom side. In the second experiment, we generate the data from the Dirichlet problem for the conductivity equation (3.1) in  $\Omega$  subject to  $u_2 = \cos(x/2) \cosh((y+1)/2)$  on  $\partial\Omega$ . Then  $f = u|_{\Gamma}$ ,  $g = -u_x|_{\Gamma}$  and  $|J| = \sigma|\nabla u|$ .

The Dirichlet problem in the unit square  $\Omega$  is solved by the finite-difference method on a uniform grid. The resulting five-diagonal symmetric system is solved

by a preconditioned conjugate gradient method. The second-order approximation and convergence of the finite-difference solution to the exact one follows from [15]. Once the numerical solutions are computed, the Dirichlet and Neumann conditions are found as  $u_j(x_0, y)$  and  $u_j(x_1, y)$ , ( $j = 1, 2$ ). The computation of  $|J|$  on the grid requires the numerical differentiation of the voltage potential  $u$ . However, it was observed in numerical experiments and then confirmed by Theorem 3.2 that the reconstruction algorithm is sensitive to the numerical differentiation of the voltage potential. To ensure the appropriate accuracy, Stechkin's optimal regularizing operators (see, e.g., [3]) are used. The shaded surfaces of  $|J|$  for the two experiments are shown in Figure 2.

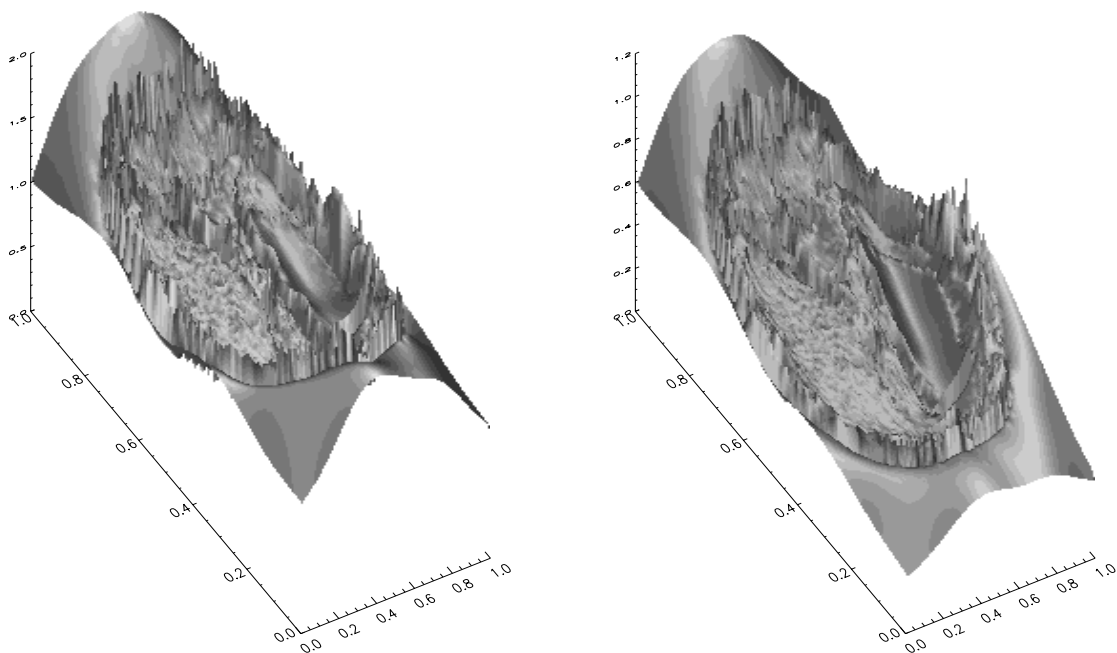


**Figure 2.** The shaded surfaces of magnitudes  $|J|$  used in the first (left) and second (right) experiments.

#### 4.2. Inversion of simulated data

The reconstruction of the conductivity distribution  $\sigma(x, y)$  is accomplished in four steps.

*Step 1. Data preparation.* The parameterized initial conditions

$$\beta(t) = f^{-1}(t), \alpha(t) = \frac{g}{f'} \circ f^{-1}(t)$$

are given for  $t \in [\underline{t}, \bar{t}]$ , where  $\bar{t} = f(1)$  and  $\underline{t} = f(0)$ . To invert the boundary data, we first do an interpolation and then swap the argument with the function values. Finally, we compute  $\nabla \ln |J|$  from the magnitude  $|J|$  on the grid by Stechkin's optimal regularizing operators.

*Step 2. Picard successive approximations.*

The Cauchy problem (2.8), (3.2) is solved by the Picard method for the operator

$$Tp(x, t) = \alpha(t) + \int_0^x \mathcal{F} \left( s, p(s, t), \beta(t) + \int_0^s p(r, t) dr \right) ds, \quad (4.1)$$

where

$$\mathcal{F}(s, u, v) = -(u^3 + u)\partial_x \ln |J|(s, v) + (u^2 + 1)\partial_y \ln |J|(s, v).$$

The function  $p(x, t)$  is a fixed point of  $T$  if and only if the function  $\psi(x, t) = \beta(t) + \int_0^x p(s, t) ds$  is the solution of the Cauchy problem (2.8), (3.2).

Some of the early successive approximations may yield curves which do not lie entirely in  $\Omega$ . For computational purposes we have extended the field  $|J|$  continuously to a larger domain. The successive approximations are known to converge to geodesics lying in  $\Omega$ , which are the solutions of (2.8) depending only on the values of  $|J|$  inside  $\Omega$ .

Given  $\alpha(t_k)$ ,  $\beta(t_k)$  for  $t_k \in [\underline{t}, \bar{t}]$  and  $\nabla \ln |J|$  on the grid, we compute the discrete function  $p(x_j, t_k)$  for  $(x_j, t_k) \in [0, \alpha] \times [\underline{t}, \bar{t}]$  by Picard successive approximations

$$p_{n+1} = T(p_n), \quad (n = 0, 1, 2, \dots).$$

The initial approximation was chosen as

$$p_0 = \begin{cases} \alpha(t_k) & \text{at } x_0 \\ \bar{\varepsilon} > 0 & \text{for } x_j \in (0, H], \end{cases}$$

where  $H \in (0, 1]$ . To advance in the interval  $(0, H]$ , we use the recurrences

$$I_n(x_{j+1}) = I_n(x_j) + I_n(\Delta x), \quad (j = 1, 2, \dots, \bar{j}),$$

where

$$I_n(x) = \int_0^x \mathcal{F} \left( s, p(s, t), \beta(t) + \int_0^s p(r, t) dr \right) ds, \\ \Delta x = x_{j+1} - x_j.$$

The value of  $\nabla \ln |J|$  at each point  $(s, t_k)$  is determined by a bilinear interpolation of precomputed  $\nabla \ln |J|$  on the grid. Note that the successive approximations converge uniformly with respect to the  $t$ -variable because of the contraction property of  $T$  in  $C[0, 1]$  with the weighted Bielecki norm

$$\|p\|_\lambda = \sup_{x \in [0, 1]} |p(x, t) e^{-\lambda x}|,$$

for a sufficiently large  $\lambda > 0$  (see, e.g., [14]).

*Step 3. Determining  $\psi(x, t)$ .* Given  $p(x_j, t_k)$  and  $\beta(t_k)$ , we compute  $\psi(x_j, t_k)$  from the finite-difference analogue of the formula

$$\psi(x, t) = \int_0^x p(s, t) ds + \beta(t).$$

The characteristics  $\psi(x, t)$  for some values of the parameter  $t$  are shown in Figure 3

*Step 4. Recovering  $\sigma$ .* Given  $\psi(x_j, t_k)$  and  $|J|$ , we compute  $\sigma$  in the region bounded by the characteristics originating from  $\Gamma$ . Since  $u(x_j, y_i) = \psi^{-1}(x_j, \cdot)(y_i)$ , the inversion

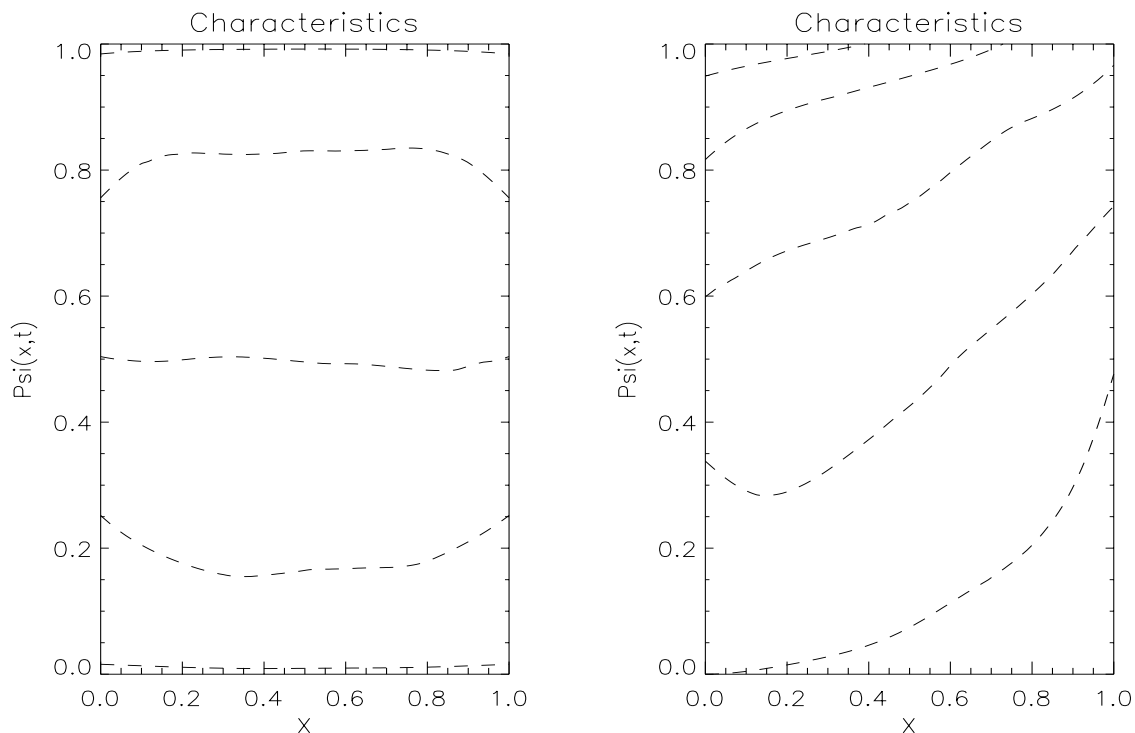


**Figure 3.** Characteristics computed in the unit square  $\Omega$  in the first (left) and second (right) experiments.

is performed by interpolating and swapping as indicated in the step 1. The discrete analogue of  $\sigma(x, y)$  is computed as

$$\sigma(x_j, y_i) = \frac{|\hat{J}|}{\sqrt{u_x^2 + u_y^2}}.$$

#### 4.3. Results

To simulate noisy data, both the Cauchy and current density data were perturbed by adding Gaussian pseudo-random vectors with zero means. The standard deviations were chosen to provide the preassigned level of errors of 1% in the Cauchy data and 5% in the current density. Such numbers correspond to the typical level of noise in measurements of the voltage potential and FID (Free Induction Decay) signals in MRI systems.

Figure 4 shows the conductivity recovered from the data associated with first model. In this case, the characteristics span the entire domain  $\Omega$  (see Figure 3 (left)). Therefore, the conductivity is uniquely reconstructed in  $\Omega$ . Figure 5 shows the conductivity recovered from the data associated with the second model. In this case, the characteristics do not span the entire region  $\Omega$ , specifically, the right lower corner is not covered (see Figure 3 (right)). Therefore, the reconstruction in this area is meaningless.

Also, the results of recovering the conductivity from noisy data show the stability



**Figure 4.** The conductivity images reconstructed from the noiseless (left) and noisy (right) data simulated in the first experiment.

of the reconstruction algorithm.

## 5. Conclusions

We have formulated the problem of conductivity imaging from one voltage-current measurement on a part of the boundary and knowledge of the magnitude of one interior current density field.

In two dimensional inhomogeneous isotropic models, the conductivity can be recovered in a specified region. In general, this region depends on the boundary and internal data. We have identified a simple sufficient condition on the Dirichlet data which guarantees that the conductivity will be recovered in the entire domain. Since the proofs are constructive, we have also developed a reconstruction algorithm. The inversion and stability results are based on classical arguments on the existence and stability of solutions of ordinary differential equations. The computational feasibility of the reconstruction algorithm has been demonstrated in numerical experiments with a simulated conductivity distribution of a human torso. The resulting images show very good resolution throughout the domain, even though they are based on a single measurement.



**Figure 5.** The conductivity images reconstructed from the noiseless (left) and noisy (right) data simulated in the second experiment.

## Acknowledgments

We thank Professor J. K. Seo for providing us with the CT-image of a human torso.

## References

- [1] Allesandrini G 1987 Critical points of solutions of elliptic equations in two variables *Ann. Scuola Norm. Sup. Pisa Cl. Sci. IV* **14** 229 – 256
- [2] Agmon S, Douglis A and Nirenberg L 1959 Estimates near the boundary for solutions of elliptic partial differential equations satisfying general boundary conditions *Comm. Pure Appl. Math.* **12** 623–727
- [3] Arestov V V 1999 Approximation of unbounded operators by bounded operators and related extremal problems *Russian Math. Surv.* **51** 1093–1126
- [4] Bers L, John F, and Schlechter M 1964 *Partial Differential Equation* (New York: Wileys)
- [5] Cheney M and Isaacson D 1991 An overview of inversion algorithms for impedance imaging *Contemp. Math.* **122** 29–39
- [6] Coddington E A and Levinson N 1955 *Theory of Ordinary Differential Equations* (New York: McGraw-Hill)
- [7] Do Carmo 1992 *Riemannian Geometry* (Boston: Birkhauser)
- [8] Hartman P 1982 *Ordinary Differential Equations* (Boston: Birkhauser)
- [9] Mandache N 2001, Exponential instability in an inverse problem for the Schrödinger equation *Inverse Problems* **17** 1435–1444
- [10] Joy M L, Nachman A I, Hasanov K F, Yoon R S, and Ma A W 2004, A new approach to Current Density Impedance Imaging (CDII), *Proceedings ISMRM, #2356* (Kyoto, Japan)

- [11] Kim S, Kwon O, Seo J K, and Yoon J R 2002 On a nonlinear partial differential equation arising in magnetic resonance electrical impedance tomography *SIAM J. Math. Anal.* **34** 511–526
- [12] Kwon O, Woo E J, Yoon J R, and Seo J K 2002 Magnetic resonance electric impedance tomography (MREIT): Simulation study of J-substitution algorithm *IEEE Trans. Biomed. Eng.* **49** 160–167
- [13] Lee J Y 2004 A reconstruction formula and uniqueness of conductivity in MREIT using two internal current distributions *Inverse Problems* **20** 847–858
- [14] Rus A 2003 Picard operators and applications *Sci.Math.Jpn.* **58** 191–219.
- [15] Samarskii A A 2001 *The Theory of Difference Schemes* (Ney York: Marcel Dekker)
- [16] Scott G C, Joy M L, Armstrong R L, and Henkelman R M 1991 Measurement of nonuniform current density by magnetic resonance *IEEE Trans. Med. Imag.* **10** 362–374
- [17] Schulz F 1990 *Regularity Theory for Quasilinear Elliptic Systems and Monge-Ampere Equations in Two Dimensions* (New-York: Springer-Verlag)
- [18] Vekua I N 1962 *Generalized Analytic Functions* (Massachusetts: Addison Wesley)